

# The Jamming Perspective on Wet Foams

Gijs Katgert

School of Physics & Astronomy and SUPA, The University of Edinburgh,  
The Kings Buildings, Mayfield Road, Edinburgh EH9 3JZ, United Kingdom.

Brian P. Tighe

Instituut-Lorentz, Universiteit Leiden, Postbus 9506, 2300 RA Leiden, The Netherlands.

Martin van Hecke

Kamerlingh Onnes Laboratorium, Universiteit Leiden, Postbus 9504, 2300 RA Leiden, The Netherlands.  
mvhecke@physics.leidenuniv.nl

## Abstract

Amorphous materials as diverse as foams, emulsions, colloidal suspensions and granular media can *jam* into a rigid, disordered state where they withstand finite shear stresses before yielding. The jamming transition has been studied extensively, in particular in computer simulations of frictionless, soft, purely repulsive spheres. Foams and emulsions are the closest realizations of this model, and in foams, the (un)jamming point corresponds to the wet limit, where the bubbles become spherical and just form contacts. Here we sketch the relevance of the jamming perspective for the geometry and flow of foams — and also discuss the impact that foams studies may have on theoretical studies on jamming.

We first briefly review insights into the crucial role of disorder in these systems, culminating in the breakdown of the affine assumption that underlies the rich mechanics near jamming. Second, we discuss how crucial theoretical predictions, such as the square root scaling of contact number with packing fraction, and the nontrivial role of disorder and fluctuations for flow have been observed in experiments on 2D foams. Third, we discuss a scaling model for the rheology of disordered media that appears to capture the key features of the flow of foams, emulsions and soft colloidal suspensions. Finally, we discuss how best to confront predictions of this model with experimental data.

## 1 Introduction

Amorphous materials as diverse as foams, emulsions, colloidal suspensions and granular media can *jam* into a rigid, disordered state where they withstand finite shear stresses before yielding [Liu and Nagel (1998); O’Hern et al. (2003); Liu and Nagel (2010); van Hecke (2010)]. The jamming transition has been studied extensively, in particular in computer simulations of frictionless, soft, purely repulsive spheres. Foams and emulsions are the closest realizations of this model, and in foams, the (un)jamming point corresponds to the wet limit, where the bubbles become spherical and just touch. What does jamming tell us about foams? And what do experiments on foams teach us about jamming?

Liquid foams and emulsions are dispersions of gas bubbles or droplets in a immiscible (second) liquid phase, stabilized by surfactants. Phenomenologically, these materials exhibit plastic

flow under large stresses, but behave elastically under small stress - their macroscopic response to mechanical perturbations is a complex mix of elastic, plastic and viscous effects [Höhler and Cohen-Addad (2005)] - as is the case for many other disordered soft materials ranging from colloidal suspensions to granular materials [Larson (1999)].

How should we think about the mechanics of such materials, and more specifically, about the mechanics of foams? More precisely, how are the laws that govern the local dynamics of bubbles and soap films related to the macroscopic, collective behavior of a foam? It is useful to introduce two extreme points of view here first, being fully aware that most researchers' views are more subtle.

One extreme point of view would be that a complete knowledge of the local mechanics is sufficient to capture the global behavior - from this perspective, the translation from local to global behavior is nothing but a straightforward coarse-graining procedure, and nontrivial collective behavior, such as nonlinear rheology, always finds its root cause in similar nontrivial local events, such as a nonlinear viscous friction law. For reasons that will become clear, we refer to this as the 'affine' picture.

Another extreme point of view would be that none of the local details matter and that the global behavior of disordered media, and foams in particular, is set by "universal" collective mechanisms [Cates et al. (1997); Olsson and Teitel (2007); Argon (1979); Falk and Langer (1998)]. Hence knowledge of the detailed interactions is irrelevant, and different local interactions, such as different local friction laws, may lead to the same macroscopic behavior, i.e. rheology.

Here we put forward a third point of view: qualitatively new behavior can emerge at the global level, but local details still may matter. So, in our view, there is no universality in the sense that changes in the microscopics often lead to changes in the macroscopic properties. However, due to the general 'non-affine' and strongly fluctuating nature of the mechanics of disordered systems, the translation from the local to the global level can be also highly nontrivial. We suggest that the *mechanisms* that connect the micro and macro world are universal. As an example of such a robust mechanism, we will discuss the role of the strength of the dynamic fluctuations, which in turn depend on the wetness of the foam and the flow rate.

We will illustrate our point of view by discussing recent experimental and numerical work on foams, and by making explicit contact with the jamming framework that has been emerging in recent years. Jamming refers to the creation (or loss) of rigidity in disordered systems in general, but the most studied models in jamming are close to models for wet foams and actually were inspired by earlier foam work [Bolton and Weaire (1990); Durian (1995)].

The outline of this paper is as follows. In section 2 we discuss the basic jamming scenario for foams, including the differences between the mechanics of disordered foams and ordered models — we conclude that disorder leads to strong non-affinity, which becomes increasingly dominant near jamming. In section 3 we discuss our recent observations of the nontrivial scaling law that relates contact number and packing fraction of foams and jammed materials — this scaling law was first seen in simulations twenty years ago [Bolton and Weaire (1990)], and has now finally been observed in 2D foams [Katgert and van Hecke (2010)]. Section 4 deals with our recent observations of the difference in rheology between ordered and disordered foams, and evidences both a nontrivial rheology for disordered 2D foams and a nontrivial scaling of the dynamic fluctuations [Katgert et al. (2008); Möbius et al. (2010)]. In section 5 we sketch the outlines of a model for the rheology of disordered media near jamming that we recently introduced [Tighe et al. (2010)] which reproduces the experimental observations discussed in section 4 well. In section 6 we briefly outline how best to confront our predictions with experimental data, and we close with a short discussion and outlook.

## 2 Jamming and Non-affinity: Consequences of Disorder

**Jamming Scenario for Foams** — Some of the earliest studies that consider the question of rigidity of packings of particles concern the loss of rigidity in foams and emulsions with increasing wetness [Princen (1983); Princen and Kiss (1986); Kraynik (1988)]. The gas fraction  $\phi$  plays a crucial role in determining the foam’s structure and rigidity. The interactions between bubbles are repulsive and viscous, and static foams are similar to the frictionless soft spheres used in most models for jamming. In real foams, gravity (which causes drainage) and gas diffusion (which causes coarsening) may play a role, although these effects can be minimized by studying quasi-2D foams and using inert gases [Weaire and Hutzler (1999)].

The (un)jamming scenario for foams is illustrated in Fig. 1. When the gas fraction approaches one, the foam is called dry. Application of deformations causes the liquid films to be stretched, and the increase in surface area then provides a restoring force: dry foams are jammed. When the gas fraction is lowered and the foam becomes wetter, the gas bubbles become increasingly spherical, and the foam loses rigidity for some critical gas fraction  $\phi_c$  where the bubbles lose contact (Fig. 1). The unjamming transition is thus governed by the gas fraction, which typically is seen as a material parameter. For emulsions the same scenario arises [Mason et al. (1995)].

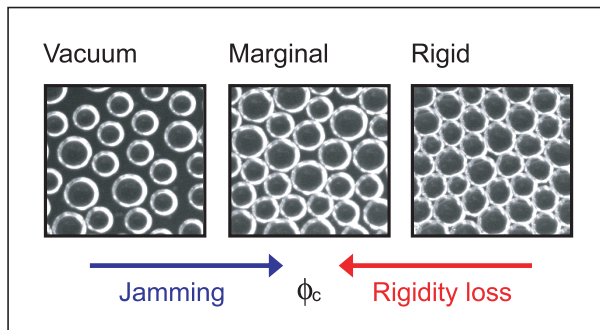


Figure 1: Topviews of 2D foams, consisting of a mix of 2 and 3 mm bubbles trapped below a top plate. At low packing fractions (left), the bubbles do not form contacts and the materials is in a mechanical vacuum state. At high packing fractions (right), the bubbles are squeezed together and form a jammed, rigid state. At intermediate packing fractions, the bubbles just touch and form a marginal state.

**Elasticity of Disordered Media** — Foams and emulsions typically form highly disordered packings. Is this disorder important for the mechanical properties, and if so, how can one deal with it?

The simplest approach is to ignore disorder altogether and start from ordered, “crystalline” packings. Tacitly assuming that all bubbles experience the same deformation, analytical calculations are then feasible, because one only needs to consider a single bubble and its neighbors to capture the foams’ geometry and mechanical response.

A famous example are two-dimensional hexagonal packings of monodisperse bubbles (“liquid honeycombs” [Princen (1983); Kraynik (1988)]). The only control parameter is then the liquid fraction of the foam or, alternatively, the packing fraction of the gas bubbles  $\phi$  (the sum of liquid fraction and packing fraction is one).

The most striking features of these liquid honeycombs are as follows. (i) The bubbles lose contact at the critical density  $\phi_c$  equal to  $\frac{\pi}{2\sqrt{3}} \approx 0.9069$ , and ordered foam packings are jammed

for larger densities. (ii) When for such a model foam  $\phi$  is lowered towards  $\phi_c$ , the yield stress and shear modulus remain finite and of similar order, and jump to zero precisely at  $\phi_c$ . (iii) The contact number (average number of contacting neighbors per bubble) remains constant at 6 in the jammed regime. Similar results can be obtained for three-dimensional ordered foams, where  $\phi_c$  is given by the packing density of the HCP lattice  $\frac{\pi}{3\sqrt{2}} \approx 0.7405$  [Höhler et al. (2008)].

Confronted with experiments on foams and emulsions, or numerical experiments on disordered foams, all three of these predictions fail! First, the critical packing fraction is substantially lower, around 84% in 2D and 64% in 3D [Bolton and Weaire (1990); Durian (1995); Mason et al. (1995); Saint-Jalmes and Durian (1999); Lespiat et al. (2011)]. The fact that the critical packing density for ordered systems is higher than that for disordered systems may not be a surprise, given that the bubbles are undeformed spheres at the jamming threshold, and it is well known that ordered sphere packings are denser than irregular ones [Weitz (2004)].

Second, the yield stress and shear modulus vanish smoothly when the critical packing fraction is reached. Early evidence comes from measurements for polydisperse emulsions by Princen and Kiss (1986), who observed a substantial lowering of the shear modulus when  $\phi$  is lowered. Later measurements by Mason et al. (1995, 1996, 1997) and Saint-Jalmes and Durian (1999) of the shear modulus and osmotic pressure of compressed disordered emulsions and foams found similar behavior for the loss of rigidity. When scaled appropriately with the Laplace pressure, which sets the local “stiffness” of the droplets, the shear modulus grows continuously with  $\phi$  and vanishes at  $\phi_c \approx 0.635$ , which corresponds to random close packing in three dimensions. There is also ample numerical evidence for this [Bolton and Weaire (1990); Durian (1995); O’Hern et al. (2003); van Hecke (2010)] - we will come back to this below.

Third, the contact number was found to vary smoothly with packing fraction. Early evidence comes from numerical simulations by Bolton and Weaire (1990), who numerically probed how a *disordered* foam loses rigidity when its gas fraction is decreased. It was found that the contact number  $z$  decreases smoothly with  $\phi$ . At  $\phi = 1$  the contact number equals six, as expected. When  $\phi \rightarrow \phi_c$ , the contact number appears to reach the *marginal* value,  $z_c = 4$ . In related work on the so-called bubble model developed for wet foams in 1995, Durian reached similar conclusions for two-dimensional model foams, and found that the contact number indeed approaches 4(=  $2D$ ) near jamming, and observed the nontrivial square root scaling of  $z - 4$  with excess density for the first time. All these findings are consistent with what is found in closely related models of frictionless soft spheres near jamming [O’Hern et al. (2003); van Hecke (2010)].

We thus conclude that disorder plays an absolutely crucial role, and in general cannot be treated as a perturbation from the regular, ordered case.

**Non-affinity** — In the preceding subsection we presented a wealth of simulational and experimental evidence that invalidates simple predictions for the elasticity of disordered media based on intuition derived from ordered packings. The crucial ingredient that is missing is the non-affine nature of the deformations of disordered packings (Fig. 2). In an affine deformation, all the local deformations simply follow the global deformation, implying that the local motion of the particles is as if they were pinned to a rubber sheet. In a disordered system such as a foam, where particles only interact with their neighbors, the local, disordered environment is crucial. The key observation is that, while materials far away from the jamming point (Fig. 2a) exhibit deformations that are close to affine (Fig. 2b), materials closer to the jamming point (Fig. 2c) exhibit deformations that become increasingly disordered and non-affine (Fig. 2d).

The role of these non-affinities is to critically change the elastic shear modulus of jammed materials such as foams [O’Hern et al. (2003)]. The scenario is as follows: far away from jamming, the local deformations are similar to the global ones - so a 1% shear strain leads to a typical change of the local deformations that is also of the order of 1%. Since these changes of deformations are

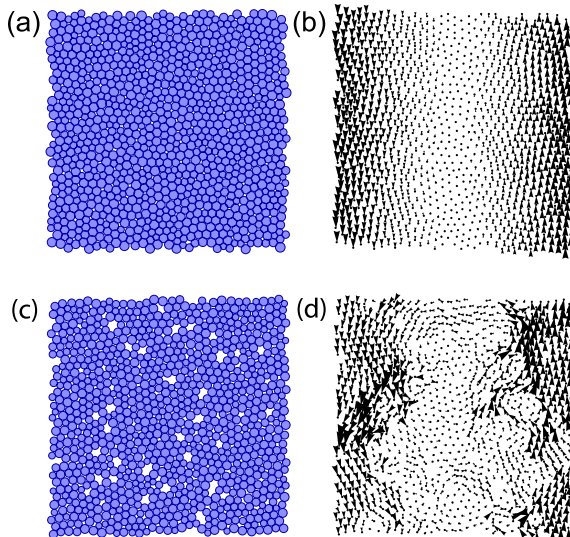


Figure 2: (a) Dense numerical bubble packing, (b) Shear response of packing depicted in (a): the bubbles move affinely and thus largely follow the imposed strain. (c) Bubble packing close to jamming and its shear response (d): The bubbles exhibit non-affine motion and swirly flow patterns.

associated with changes in the forces between bubbles/particles, and concomitant changes in the elastic energy, one can then immediately estimate the change in elastic energy once the interactions between particles are known. In particular, for linear interactions with a local spring constant  $k$ , one concludes that the shear modulus  $G$  is on the order of  $k$ , just as in the affine picture sketched above.

Closer to jamming, however, the number of contacts per bubble drops, and bubbles are increasingly free to deviate from the affine field so as to minimize the changes in elastic energy, and, as a consequence, the shear modulus  $G$  gets smaller than would be expected from an affine assumption. At the jamming point, the shear modulus vanishes for harmonically interacting particles — clearly here the translation from local to global interaction is nontrivial! For different (e.g., power law interactions such as Hertzian interactions), the shear modulus behaves differently, so there is no simple universality. However, the ratio of shear modulus to local spring constant (or equivalently, the ratio of shear modulus to bulk modulus  $K$ ) scales in a robust manner with distance to jamming: independent of dimension and interaction potential,  $G/K \propto z - z_c$ , where  $z_c$  is the number of contacts at the critical point ( $=2D$ ). [O’Hern et al. (2003); Ellenbroek et al. (2009)]. This illustrates our earlier point: local interactions matter, but there are universal and sometimes nontrivial mechanisms that translate the local interactions to the global behavior.

As there is no simple way to estimate the particle motions and deformations in disordered systems, one needs to resort to (numerical) experiments. Jamming can be seen as the avenue that connects the results of such experiments. Jamming aims at capturing the mechanical and geometric properties of disordered systems, building on two insights: first, that the non-affine character becomes dominant near the jamming transition, and second, that disorder and non-affinity are not weak perturbations away from the ordered, affine case, but may lead to completely new physics [Somfai et al. (2005); Mason et al. (1995); Radjai and Roux (2002); Tanguy et al. (2002, 2004); Lemaitre and Maloney (2006); Maloney (2006)].

### 3 Contacts and density in 2D foams near jamming

We have recently experimentally investigated the static structure of a disordered monolayer of foam bubbles that form a bidisperse packing similar to the detail shown in Fig. 3. This monolayer floats on the surface of a soapy solution and is bound on the top by a well-leveled glass plate [Katgert et al. (2008); Katgert and van Hecke (2010)]. This setup allows for direct optical access of all bubbles, in contrast to three dimensional foams, which are opaque due to multiple scattering of the interfaces. The packing fraction can be varied simply by in- or decreasing the gap between the glass plate and the soapy solution.

The question we set out to answer is whether the numerically ubiquitous scaling of the excess contact number with the square root of the excess density [Durian (1995); O’Hern et al. (2003)] could be observed in experiment. In order to probe this question we prepare many distinct packings of our bidisperse foam at fixed  $\phi$ , by stirring the bulk soapy solution to rearrange the packing. After the packings have relaxed to an equilibrium state, we take photographs of the resulting structure with a 6 megapixel camera and analyse these by advanced image analysis. Even though the bubbles are three dimensional entities, we adjust the lighting of our experiment such that we image the bubbles as two-dimensional discs, at the point where they are broadest. This approach seems to be justified, *a posteriori*. For each realization we determine the average contact number  $z$  and the packing fraction  $\phi$ , see grey dots in Fig. 3. For high packing fractions, the contact number tends to  $z = 6$ , the expected value for disordered cellular structures [Weaire and Hutzler (1999)]. However, we observe that, as the foam packing fraction is reduced, the average contact number decreases, ultimately reaching  $z_c = 4$ , at a packing fraction around  $\phi = 0.84$ . Below this value the foam loses stability. Both the value of the critical density and contact number at the unjamming point are fully consistent with predictions.

We also plot the average over all images for each packing fraction (black circles). Clearly the variation of  $z$  with  $\phi$  is similar to a square root, and to compare our data to predictions we fit our data to a power law fit of the form  $z = 4 + z_0 * (\phi - \phi_c)^\beta$  (red curve in Fig. 2). The best fit gives us  $z_0 = 4.02 \pm 0.20$ ,  $\phi_c = 0.842 \pm 0.002$  and  $\beta = 0.50 \pm 0.02$ , in remarkable agreement with theoretical predictions by O’Hern et al and Durian [O’Hern et al. (2003); Durian (1995)], who found  $z_0 = 3.6 \pm 0.5$ ,  $\phi_c = 0.841 \pm 0.002$  and  $\beta = 0.49 \pm 0.03$ .

In simulation studies the packing fraction is often calculated by counting the overlaps between bubbles *twice*. In the experiment we are restricted to extracting an area fraction from images. We therefore convert our experimentally determined packing fractions to the corresponding theoretical packing fractions. If we do not convert our experimentally determined packing fractions, we find an effective scaling exponent  $\beta = 0.70$  when plotting  $z$  as a function of  $\phi_{exp}$ , see inset of Fig. 3.

We were not the first to experimentally investigate the scaling of  $z$  with  $\phi$ . Majmudar et al. [Majmudar et al. (2007)] have extracted the same quantities from images of two-dimensional, frictional, photoelastic discs and compared these to predictions from simulations. From their data it appears the prefactor  $Z_0 \approx 16$ , inconsistent with simulations. Our results do allow for a direct comparison with predictions for *frictionless* jamming, which can be seen from the excellent agreement between parameters. We also note that Brujić et al. recently have probed this squareroot scaling in 3D emulsions (private communication).

We conclude that, as far as static structure is concerned, (2D) foams and numerical models for jamming are in excellent agreement. Disorder is crucial for real foams.

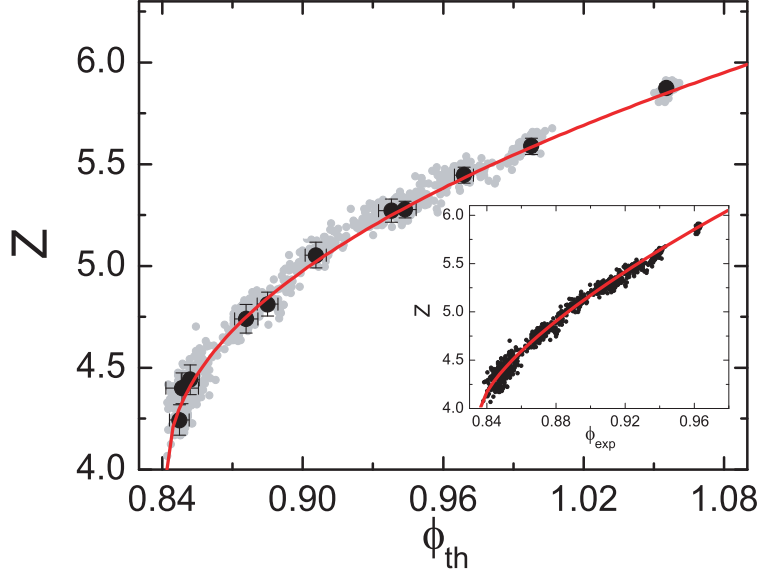


Figure 3: Average contact number versus  $\phi$  for experimental bidisperse foams: grey dots indicate data for each individual realization, black circles indicate averages for each globally set packing fraction. Solid red line is fit of the form  $z = 4 + z_0 * (\phi - \phi_c)^\beta$ , with  $z_0 = 4.02 \pm 0.20$ ,  $\phi_c = 0.842 \pm 0.002$  and  $\beta = 0.50 \pm 0.02$ . Inset is data plotted versus experimentally determined packing fraction  $\phi_{\text{exp}}$ . The fit has a power law exponent of 0.70.

## 4 Disorder and fluctuations in foam flows: Experiments

In a series of experiments [Katgert et al. (2008, 2009); Möbius et al. (2010)] we have recently probed the role of disorder in the flow of 2D foams. In these experiments, we shear a foam monolayer that is floating on a soapy solution and bound by a glass plate. We calculate averaged velocity profiles and track the bubble displacements. Our two main findings are 1) that disorder plays a crucial role in the rheology — the global rheology is very different than what you would expect based on measurements of the local drag forces — and that 2) fluctuations become increasingly strong as the strain rate is *lowered*.

**Drag forces** — To probe the role of disorder, we have compared the averaged flow profiles and bubble trajectories of a ordered, crystalline foam and a disordered, bidisperse foam (Fig. 4). For monodisperse foams (Fig. 4a), the bubbles move past each other in a ziplike fashion along the crystal planes of the hexagonal lattice formed by the bubbles, see Fig. 4b for tracks. The velocity profiles (Fig. 4b) are strongly localized and are independent of driving velocity. For disordered foams (Fig 4c) the situation is vastly different: the bubble motion becomes disordered and organizes into the swirly, collective patterns typically seen in materials near jamming, see Fig 4d. The velocity profiles now depend on the driving velocity, and become increasingly delocalized as the driving velocity is decreased.

To understand the flow profiles, we introduce a simple force balance model in which the averaged viscous friction between bubbles that move past each other,  $F_v$ , is balanced by the viscous friction due to the bubbles moving past the glass plate,  $F_{bw}$  [Janiaud et al. (2006); Katgert et al. (2008, 2009)]. We note here that without the top plate, the flow profiles are essentially linear [Wang et al. (2006)] — the shear banding seen here is thus simply due to the top plate [Janiaud et al. (2006); Schall and van Hecke (2010)]. We check rheometrically that the top plate drag is given

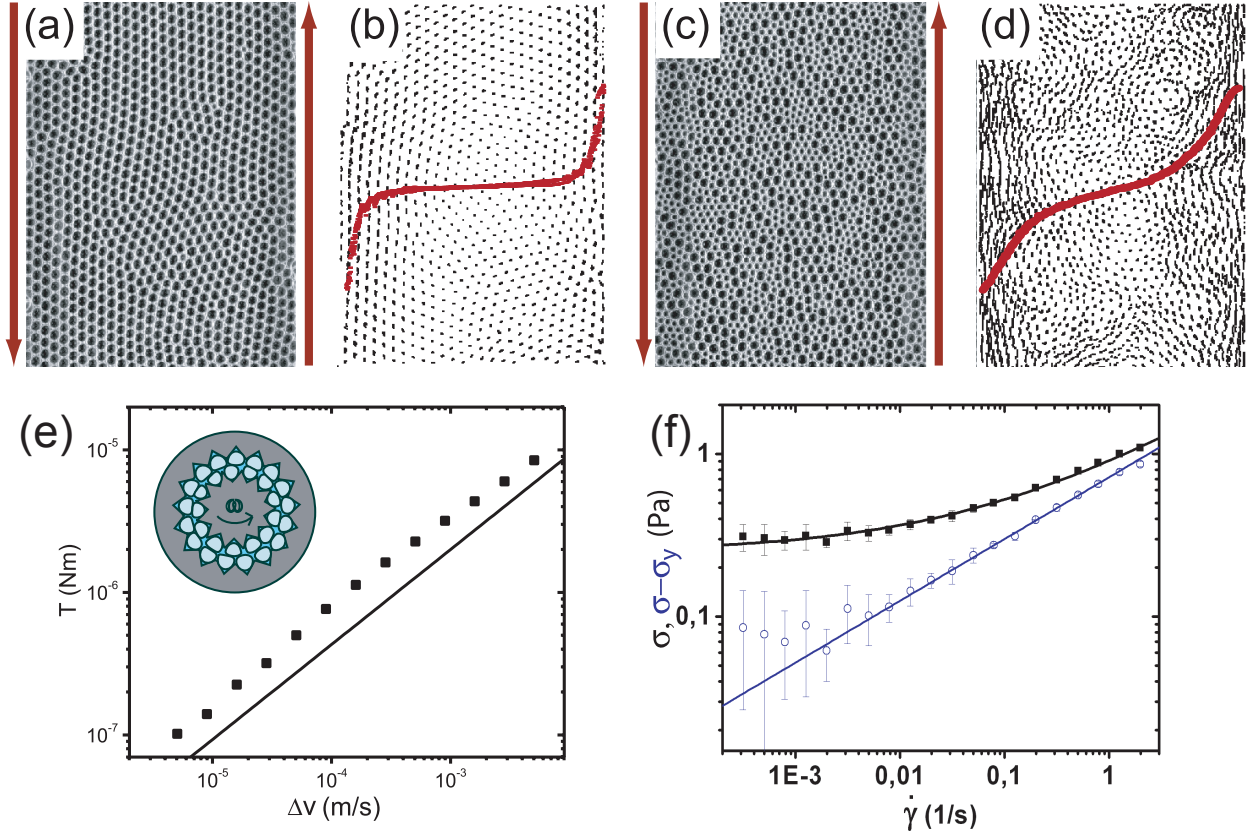


Figure 4: (a) Top view of linearly sheared monodisperse foam. Arrows indicate direction of shear at the boundaries. (b) Bubble tracks for monodisperse foam in (a): bubbles slide along planes thus move affinely; the resulting velocity profiles are strongly localized (red curve). (c) Bidisperse foam, and its corresponding bubble tracks (d): swirly, non-affine motion is clearly visible, and the velocity profile exhibits less localization. Ingredients into the model describing these flows: (e) Viscous friction between to *ordered* bubble rows (see inset) as a function of  $\Delta v$ . Solid line  $\sim \Delta v^{2/3}$ . (f) Stress-strain rate relation for *disordered* two-dimensional foam: black solid line indicates fit to the Herschel-Bulkley expression:  $\sigma = \sigma_y + A\dot{\gamma}^\beta$ , with  $\beta = 0.36$ . This power law scaling is highlighted by subtracting the yield stress  $\sigma_y$  (blue data).

by the classic result of Bretherton  $F_{bw} \sim v^{2/3}$  [Bretherton (1961)]. We then extract the scaling of interbubble friction  $F_v$  with velocity gradient by fitting the model to the velocity profiles.

Our model predicts rate independent velocity profiles, as seen in the ordered foam, only if the interbubble viscous friction scales in the same way as the bubble-wall friction:  $F_v \sim \Delta v^{2/3}$ , where  $\Delta v$  is the velocity difference between neighboring bubbles. We verify this scaling with rheological measurements on two ordered bubble layers gliding past each other, and find that the bare viscous friction between bubbles moving past each other indeed scales in exactly the same way with the velocity difference between bubbles as the frictional force between bubble and top plate, see Fig. 4e. Hence, the rate-independence of the observed flow profiles for ordered foams indicates that the local viscous drag law immediately and trivially sets the global drag forces.

For the disordered foams, the remarkable thing is that their rate dependent profiles are consistent with the force balance model if the exponents for bubble-bubble and bubble-wall friction are *different*. In fact, we excellently fit all our velocity profiles by our model with a bubble-wall friction as dictated by Bretherton’s result and an average interbubble friction that scales as  $\Delta v^{0.36}$ . Since the local friction law between bubbles is independent of the bubble configuration, we conclude that in this case the translation from local to global drag forces is highly nontrivial.

We have further checked this remarkable result by bulk rheometry on disordered two dimensional foam layers. Bulk foam flow curves are commonly fit with the phenomenological Herschel-Bulkley constitutive relation, linking the stress  $\sigma$  with the strain rate  $\dot{\gamma}$  :

$$\sigma = \sigma_y + A\dot{\gamma}^\beta \tag{1}$$

with  $\sigma_y$  the yield stress. In this measurement (Fig. 4f), the flow exponent  $\beta = 0.36$ , consistent with our indirect determination of  $\beta$  via the flow profiles. We thus find that disorder changes the effective viscous friction between bubbles in a highly nontrivial way: the averaged viscous dissipation inside the foam is enhanced with respect to the ordered case, leading to less localized and rate dependent flows.

In the next section, we will present a theoretical model that fully captures the nontrivial translation from the local exponent of  $2/3$  to the global exponent of  $0.36$ .

We also point out here another difference between the measured rheology of disordered foams and ordered foams: the disordered foams have a finite yield stress ( $\sigma_y$ ), while the ordered foams exhibit pure power law scaling. As we will discuss in section V.C, this is deeply connected to the relation between fluctuations and energy dissipation in the system.

**Fluctuations** — We have also studied the bubble displacements in detail via tracking of the irregular bubble motion [Möbius et al. (2010)]. After subtracting their average velocity, we have probed their remaining erratic motion. Since we can probe local strain rates that span multiple decades, we can plot the mean squared displacement (MSD) of the bubbles as a function of local strain rate. For all strain rates we see that the MSD’s cross over from superdiffusive to diffusive behavior at a well defined relaxation time  $t_r$  that corresponds to a MSD of  $(0.14\langle d \rangle)^2$ , which is remarkably similar to the Lindemann criterion for cage breaking in colloidal suspensions [Besseling et al. (2007)].

When we extract this  $t_r$  for different local strain rates, we observe that it does *not* scale with the inverse local strain rate  $\dot{\gamma}^{-1}$ , which could have been expected since both rearrangements and fluctuations are entirely shear induced. In contrast, we find that  $t_r \sim \dot{\gamma}^{-0.66 \pm 0.05}$ . This result implies that fluctuations *increase* for slower flows, in contrast to the commonly accepted viewpoint that foam flows tend to quasistaticity when lowering the strain rate, reflected in the expected scaling  $t_r \sim \dot{\gamma}^{-1}$ . This result can be made more explicit by replotting the MSD curves as function of the accumulated strain — the lower the strain rate, the larger the MSD at given strain [Möbius et al. (2010)]. Hence fluctuations become stronger the slower the flow.

## 5 Disorder and fluctuations in foam flows: Simulations and Theory

In this section we will present a jamming-inspired, theoretical perspective on the flow of foams. For completeness, we first introduce several variants of the “bubble model”, a microscopic model suitable to simulate the flow of wet foams — readers familiar with, or not interested in the details of these models can skip this section. We then discuss the main rheological features that these models display in direct numerical simulations. We then show that a basic energy balance equation implies that the relative strength of fluctuations *grows* for decreasing flow rates, and actually *diverges* in

the limit of zero flow rate - consistent with the experimentally observed growth of the diffusivity discussed above. We finally outline the main contours of a model for the rheology of soft materials, such as foams, near jamming. This model combines recent insights on elasticity near jamming with our observations on the nature of the fluctuations, and predicts several scaling regimes that should be, and partly have been, observed in the flow of foams.

## 5.1 Computer Models for Foam Flow

There are various versions of microscopic models suitable for simulating the flow of wet foams (and other disordered media). All version we will discuss here stem from the “bubble model” introduced in 1995 by Durian [Durian (1995)]. In these models, all bubbles are represented by soft spherical (disk-like in 2D) particles, that only interact when in contact. Following Durian, it is typical to take the equations of motion to be overdamped [Durian (1995, 1997); Ono et al. (2002); Tewari et al. (1999); Olsson and Teitel (2007); Tighe et al. (2010)], an appropriate approximation for slow flows in which damping dominates inertia. This formally corresponds to the limit in which bubble masses are set to zero, and hence at any instant the elastic and viscous forces on each bubble balance. Other authors elect to retain inertial terms in the equations of motion [Hatano (2008); Langlois et al. (2008); Otsuki and Hayakawa (2009)]; in the underdamped limit this produces a qualitatively different rheology.

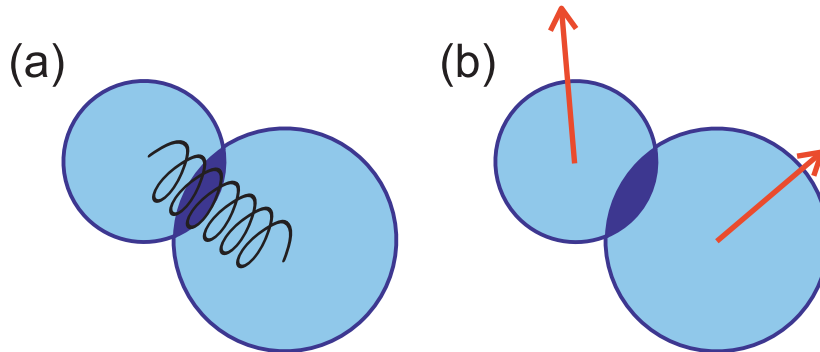


Figure 5: (a) Elastic and (b) viscous forces between bubbles in the bubble model: when bubbles overlap, the strength of their mutual repulsion is a function of the overlap — the bubbles act as one-sided springs. The viscous forces are taken to be a function of the velocity difference between bubbles sliding past each other.

To specify a particular variant of the bubble model one must describe the elastic and viscous forces between bubbles. Elastic forces are typically taken to be generated by harmonic “one-sided springs”, see Fig. 5a. These springs have rest lengths equal to the sum of the contacting bubbles’ radii; their one-sidedness refers to the fact that they apply a force only when the spring is compressed, thereby guaranteeing that the elastic forces are purely repulsive. Another common force law is the Hertzian interaction, which describes emulsions rather than foams [Lacasse et al. (1996)]. A “Hertzian spring” is also one sided, but its repulsive force grows as the 3/2 power of the spring’s compression. In general, then,

$$f_{\text{el}} \sim \delta^{\alpha_{\text{el}}}, \quad (2)$$

where  $\delta$  is the dimensionless compression of the spring and  $\alpha_{\text{el}} = 1$  (3/2) corresponds to harmonic

(Hertzian) forces — for the simulations we describe below  $\alpha_{\text{el}} = 1$ .

Similarly, it is natural to invoke a viscous force law in which the relative velocity of contacting bubbles is damped (Fig 5b):

$$\begin{aligned} f_{\text{visc}}^{\parallel} &= b^{\parallel}(\Delta v^{\parallel})^{\alpha_{\text{visc}}} \\ f_{\text{visc}}^{\perp} &= b^{\perp}(\Delta v^{\perp})^{\alpha_{\text{visc}}}. \end{aligned} \quad (3)$$

For the simulations we describe below  $\alpha_{\text{visc}} = 1$ , which corresponds to linear viscous dissipation. Real foams, however, are believed to have  $\alpha_{\text{visc}} < 1$ , with the actual value depending on the surfactant used [Denkov et al. (2009)]. For the mobile surfactants used in the experiments described above, our measurements indicate  $\alpha_{\text{visc}} = 2/3$ , see Fig. 4(e). We shall see that changes in the microscopic exponent  $\alpha_{\text{visc}}$  have measureable ramifications for the macroscopic rheology. We also take  $b^{\parallel} = b^{\perp}$ , so that the dissipation is indifferent to whether the particles are moving together, moving apart, or sliding. Other authors have taken  $b^{\perp} = 0$ , so that sliding does not dissipate [Hatano (2010); Otsuki and Hayakawa (2009)], though this case may be pathological.

Finally we point out that there is another, qualitatively different, viscous force law commonly used in the literature [Durian (1995, 1997); Ono et al. (2002); Tewari et al. (1999); Olsson and Teitel (2007)]. Known as “mean field” dissipation, it specifies that each bubble experiences a damping force proportional to the difference between its instantaneous velocity and the *mean* velocity  $\vec{v}_{\text{lin}} = \dot{\gamma}x \hat{y}$  of a bubble at its position:

$$\vec{f}_{\text{MF}} = -b_{\text{MF}}(\vec{v} - \vec{v}_{\text{lin}}). \quad (4)$$

This expression assumes the linear velocity profile established by Lees-Edwards boundary conditions. It sacrifices more realistic modeling for numerical convenience: in overdamped dynamics, Eq. (4) can be simulated far more efficiently than Eq. (3).

## 5.2 Phenomenology

In the static limit, all microscopic models introduced above reduce to the simple models that are studied to probe elastic properties near the jamming transition. Most crucial, in order for the material to have a finite rigidity, they need to be packed at a sufficiently large packing fraction — the critical packing fraction corresponds to extremely wet foams where the bubbles just touch. Once such packings are created, they are subjected to a fixed strain rate and the shear stress can be measured numerically — in some cases, the stress has been fixed and the strain rate has been measured [Olsson and Teitel (2007)], but in all cases, flow profiles have been found to be simply linear (i.e., no shear banding — when we include additional drag terms, modeling interactions with a top plate, the same shear banding that is seen experimentally is recovered).

There are certain generic features of the macroscopic rheology that prevail for  $\phi > \phi_c$  in simulations of any version of the bubble model discussed above. Namely, the constitutive relation is qualitatively similar to the Herschel-Bulkley constitutive relation defined in Eq. (1)<sup>1</sup>. The exponent  $\beta$  is typically less than one, a property known as “shear thinning.” In numerics one observes that  $\sigma_y$  varies with  $\phi$  and vanishes at  $\phi_c$ , which motivates us to write  $\sigma_y \sim \Delta\phi^{\Delta}$  for some  $\Delta$ . Note that because  $\sigma = \sigma_y$  in the limit  $\dot{\gamma} \rightarrow 0$ , it is natural to expect that the exponent  $\Delta$  depends on  $\alpha_{\text{el}}$  but *not* on  $\alpha_{\text{visc}}$ , a dynamical quantity. By contrast  $\beta$  is a dynamical exponent which will turn out to depend on both  $\alpha_{\text{visc}}$  and  $\alpha_{\text{el}}$ . The challenge is to identify how  $\Delta$ ,  $A$ , and  $\beta$  depend on the microscopic details of the model.

---

<sup>1</sup>We note here that we do not believe that the flow curves are exactly of this form, although this is almost always a good approximation

### 5.3 Fluctuations

Slow foam flows are dominated by fluctuations. For example it is widely believed that the main contribution to dissipation in dry foams stems from localized neighbor-swapping, or T1, events [Höhler and Cohen-Addad (2005)]. Here we focus on the wet limit, where T1 events are not well defined. Nevertheless, here again there is a precise relation between the fluctuations and dissipation.

**Power balance** — If one shears a foam (or any other system) at a rate  $\dot{\gamma}$ , and it resists this flow with a shear stress  $\sigma$ , the product of the two gives the average rate of work done on the system. This work has to be dissipated, and for wet foams the only dissipative mechanism is the relative motion of neighboring bubbles. Let us first take a simple model, where the viscous force  $f_{visc}$  between bubbles is proportional to their relative velocity  $\Delta v$ . In a time interval  $\Delta t$ , the amount of energy dissipated per pair of sliding bubbles is then  $f_{visc} \times \Delta t \times \Delta v$ , which scales as  $\Delta v^2 \Delta t$ . The crucial observation is that the energy fed into the system by shear needs to be balanced by the amount of energy dissipated by local bubble sliding:

$$\sigma \dot{\gamma} \sim \langle \Delta v^2 \rangle, \quad (5)$$

where the brackets denote averaging over the system <sup>2</sup>.

We now show the powerful consequences of this simple relation. Let us first imagine that our foam behaves as a Newtonian fluid, for which  $\sigma = \eta \dot{\gamma}$ . In that case the steady state power balance equation Eq. (5) requires that the  $\eta \dot{\gamma}^2 \sim \langle \Delta v^2 \rangle$ , so that  $|\Delta v|$  and  $\dot{\gamma}$  scale in the same way.

However, foams do not behave as Newtonian fluids, particularly for slow flows. Let us assume that the stress varies as a power law of the strain rate, which is a good approximation of a typical Herschel-Bulkley rheology at high flow rate:  $\sigma \sim \dot{\gamma}^\beta$ . Substituting this into the steady state power balance equation, Eq. (5), one obtains  $\dot{\gamma}^{1+\beta} \sim \langle \Delta v^2 \rangle$ , so that  $|\Delta v|$  and  $\dot{\gamma}$  *do not* scale in the same way; rather  $|\Delta v| \sim \dot{\gamma}^{(1+\beta)/2}$ . For the typical case that  $\beta < 1$ , one concludes that the velocity fluctuations decay sublinearly with strain rate, or in other words, that the *relative* velocity fluctuations,  $|\Delta v|/\dot{\gamma}$  diverge as  $\dot{\gamma}^{(\beta-1)/2}$ . This divergence is even stronger for slow flows for which the stress reaches a plateau value:  $\sigma \approx \sigma_y$ . The steady state power balance equation Eq. (5) then predicts  $|\Delta v|/\dot{\gamma}$  to diverge as  $\dot{\gamma}^{-1/2}$ .

The divergence of the fluctuations suggests that there is no well-defined quasistatic limit, at least not as far as the trajectories of the bubbles are concerned: the slower you go, the bigger the fluctuations. Imagine you are given two movies of foam flows at two different flow rates — but you are not told which one is the fastest, nor do you know the frame rate of these movies. By adjusting their playback speed, you can make the average flow rate of the two movies equal — the energy balance argument predicts that the amount of fluctuations would be largest in the movie corresponding to the slowest flow. We stress here that, at least qualitatively, this is precisely what we observed in the experiments on diffusion of foam bubbles in flow.

**Characteristic Scales** — The fluctuations introduce a nontrivial dynamical time scale into the problem:  $t_{\text{dyn}} = d/|\Delta v|$ , where  $d$  is a typical bubble diameter — this time can be thought of as characterizing the time scale over which local rearrangements take place. In the simplest case of a Newtonian fluid, for which  $|\Delta v| \sim \dot{\gamma}$ ,  $t_{\text{dyn}}$  is nothing more than the inverse strain rate.

For non-Newtonian fluids, however,  $\Delta v$  scales nontrivially, hence the dynamical timescale does, as well. For a pure power law fluid we find  $t_{\text{dyn}} \sim \dot{\gamma}^{(1+\beta)/2}$ , and for the yield stress case we find  $t_{\text{dyn}} \sim \dot{\gamma}^{+1/2}$ .

One can translate this time scale into a characteristic strain scale necessary to induce rearrangements:  $\gamma_{\text{dyn}} = t_{\text{dyn}} \dot{\gamma}$ . This characteristic strain thus vanishes for slow flows — the slower the flow,

---

<sup>2</sup>In all scaling arguments that will follow we focus on the typical scale of quantities, and ignore correlations — we do not believe these will change our results in an essential manner.

the smaller the overall strains necessary to induce substantial rearrangements.

**Relation between local viscous drag, fluctuations and rheology** — Let us now clarify the relations between local dissipation, fluctuations and global rheology. First, let us generalize the viscous force to be nonlinear:  $f_{\text{visc}} \propto |\Delta v|^\alpha$ . Now assume that the macroscopic rheology is of the form  $\sigma \propto \dot{\gamma}^\beta$ . The power balance equation then reads  $\dot{\gamma}^{\beta+1} \sim \langle \Delta v^{1+\alpha} \rangle$ , which will give nontrivial fluctuations whenever  $\alpha \neq \beta$ .

This shows that details matter in the sense that different local dissipative laws directly affect the precise form of the balance Eq. (5) — in this sense, the physics is not universal. On the other hand, as long as  $\beta < \alpha$ , the fluctuations become stronger for slower flow. We will see that this inequality is in general satisfied, so that the divergence of fluctuations is robust.

The balance arguments can also be used to rationalize part of our experimental findings. Recall that in rheological experiments in which two ordered rows of bubbles were slid past each other with velocity  $\Delta v$  [Katgert et al. (2008, 2009)], see Fig. 4e, the time-averaged shear stress  $\sigma$  was found to scale as a simple powerlaw:  $\sigma \sim \Delta v^\alpha$ . In particular, there was *no* force plateau at low  $\Delta v$ . In contrast, for a disordered bubble raft, the stress had a Hershel-Bulkley form with a plateau for low strain rates and a power law different from  $\alpha$ :  $\sigma \sim \sigma_0 + A\dot{\gamma}^\beta$ , see Fig. 4f.

The finite plateau we can understand as follows. As we have seen, the energy balance argument shows that for flows in the regime where the stress is on a plateau, the relative fluctuations must diverge when the strain rate goes to zero. Since the fluctuations are constrained in the ordered system, they cannot diverge, energy cannot be dissipated strongly enough, and as a result *there cannot be a yield stress* — consistent with our findings. In the disordered system, the fluctuations are not constrained, and nothing forbids the emergence of a finite yield stress.

We stress here that the role of disorder is to facilitate the nontrivial role of the fluctuations. In ordered systems, such as the ordered foams we discussed above, whole rows of bubbles slide past each other, and there is simply not enough freedom to allow for large fluctuations. In disordered systems, the bubbles have much more freedom to choose their path. For the case of elasticity of disordered media, discussed in section II, disordered bubble motion was intimately connected to anomalous scaling of the shear modulus. Here we see that for the flow of disordered media, nontrivial fluctuations are connected to anomalous scaling of the stress-strain rate relation.

The difference between the local and global rheological exponents  $\alpha$  and  $\beta$  is also intimately related to the fact that the fluctuations are rate dependent. But the single balance equation Eq. (5) is not sufficient to predict both  $\beta$  and the fluctuations — we need additional arguments to obtain a set of closed equations. In the next section we will introduce such equations, and produce a definite prediction of  $\beta$  as function of the local drag force  $\alpha$ .

## 5.4 Scaling model for foam flows

We now introduce a model that seeks to explain bubble model rheology for  $\phi > \phi_c$ . Our goal is to give the flavor of the model, without delving too far into details. For simplicity, we first fix the elastic ( $\alpha_{\text{el}}$ ) and viscous exponent ( $\alpha_{\text{visc}}$ ) to one.

The scaling model has three ingredients. These are

1. the system is in power balance
2. a flowing foam can be mapped to a static system that has been sheared through an effective strain  $\gamma_{\text{eff}}$
3. the stress as a function of  $\gamma_{\text{eff}}$  is given by the constitutive relation for sheared disordered spring networks

One of the difficulties in explaining this model is that there are several different regimes with different forms for the effective strain and stress-strain relation. We first will describe the model in two of the simplest limits, and then briefly point out how all these results can be generalized.

*Critical Regime* — In the limit of very wet foams, i.e.,  $\phi \rightarrow \phi_c$ , the model is particularly simple. We postulate that the effective strain in the system then simply equals the dynamical strain introduced above:  $\gamma_{\text{dyn}} \sim \dot{\gamma}/|\Delta v|$ . For the equation for the stress, we build on recent work that shows that near jamming, the linear shear modulus vanishes and the stress scales as  $\sigma \sim |\gamma|\gamma$ . [Wyart et al. (2008)]. Now we have a closed set of three equations (we drop all absolute values and averages):

$$\sigma\dot{\gamma} \sim \Delta v^2 . \quad (6)$$

$$\gamma_{\text{eff}} \sim \dot{\gamma}/\Delta v . \quad (7)$$

$$\sigma \sim \gamma_{\text{eff}}^2 . \quad (8)$$

We have identified  $\gamma$  with  $\gamma_{\text{eff}}$ ; this is point 3 in the above list. These equations can easily be solved and yield a prediction for the rheology of the form  $\sigma \sim \dot{\gamma}^{1/2}$ , which is in very good agreement with numerical simulations of the bubble model [Tighe et al. (2010)].

*Yield Stress Regime* — In the limit of very slow flows and for  $\phi > \phi_c$ , the model also becomes very simple. In that regime, the effective strain is no longer expected to be dominated by dynamic effects, and we postulate that the effective strain in the system then equals  $\Delta\phi := \phi - \phi_c$  [Tighe et al. (2010)]. For the equation for the stress, recent work shows that away from jamming, the shear modulus  $G$  scales with the distance to jamming as  $G \sim \Delta z \sim \sqrt{\Delta\phi}$ . In summary:

$$\sigma\dot{\gamma} \sim \Delta v^2 . \quad (9)$$

$$\gamma_{\text{eff}} \sim \Delta\phi . \quad (10)$$

$$\sigma \sim \sqrt{\Delta\phi}\gamma_{\text{eff}} . \quad (11)$$

These equations can easily be solved, and yield as prediction that the stress is a constant  $\propto \Delta\phi^{3/2}$ .

*Transition Regime* — The general form of the model is obtained by combining these regimes, so that  $\gamma_{\text{eff}} = a_1\Delta\phi + a_2\dot{\gamma}/\Delta v$ , and  $\sigma = a_3\sqrt{\Delta\phi}\gamma_{\text{eff}} + a_4\gamma_{\text{eff}}^2$ , where  $a_i$  are numerical constants to be determined. It turns out that there are three different regimes, and in all cases, either the first or the second term in these sums dominates <sup>3</sup>. The third regime we refer to as the transition regime, and here the three equations are:

$$\sigma\dot{\gamma} \sim \Delta v^2 . \quad (12)$$

$$\gamma_{\text{eff}} \sim \dot{\gamma}/\Delta v . \quad (13)$$

$$\sigma \sim \sqrt{\Delta\phi}\gamma_{\text{eff}} , \quad (14)$$

which yields that the stress scales as  $\sigma \sim (\Delta\phi)^{1/3}\dot{\gamma}^{1/3}$  — this third regime came as a complete surprise, and its existence implies deviation from the usual Herschel-Bulkley phenomenology. This deviation is difficult to observe in numerics but consistent with our observation that very often, Herschel-Bulkley-fits to experimental or numerical data underestimate the data in the crossover regime between yield stress and power law behavior - precisely the regime where the transition rheology is predicted.

By substituting the various solutions we have obtained into the general expressions for the effective strain and stress, one can do a self consistency check to see for which strain rates, which

---

<sup>3</sup>In principle there are four regimes, but the combination of terms in this fourth regime never dominate the physics — see [Tighe et al. (2010)].

regime should dominate — we find that the Yield Stress regime dominates for  $\dot{\gamma} \lesssim \Delta\phi^{7/2}$ , the Critical Regime for  $\dot{\gamma} \gtrsim \Delta\phi^2$  and the Transition regime in the range in between — which can span arbitrarily many decades when  $\Delta\phi$  tends to zero.

*General Microscopics* — What happens when the microscopic exponents ( $\alpha_{\text{el}}$ ) and ( $\alpha_{\text{visc}}$ ) are unequal to one?

For the Yield Stress regime, the stress-strain relation is affected by the value of  $\alpha_{\text{el}}$ , as it sets the scaling of the shear modulus  $G$  with  $\Delta\phi$ . Prior work has shown that for nonlinear interactions, the stress strain relation becomes  $\sigma \sim \Delta\phi^{\alpha_{\text{el}}} - 1/2$  [O’Hern et al. (2003)]. Thus the yield stress varies with  $\alpha_{\text{el}}$  according to  $\Delta = \alpha_{\text{el}} + 1/2$ . For  $\alpha_{\text{el}} = 3/2$ , believed to describe dense emulsions and microgel suspensions [Lacasse et al. (1996); Nordstrom et al. (2010a)], this gives  $\sigma_y \sim \Delta\phi^2$ , in good agreement with experimental measurements by Mason et al. (1996) and Nordstrom et al. (2010), which both find  $\Delta \approx 2$ .

For the Critical Regime, both the elastic and viscous exponent matter. Let us keep the elastic exponent equal to one, which is a good approximation for foams. Recall that  $\beta$  should, in general, depend on  $\alpha_{\text{visc}}$ . Repeating the analysis in the critical regime for arbitrary  $\alpha_{\text{visc}}$  yields

$$\beta = \frac{2\alpha_{\text{visc}}}{\alpha_{\text{visc}} + 3}. \quad (15)$$

For  $\alpha_{\text{visc}} = 2/3$ , as is the case for mobile surfactants, we obtain  $\beta = 4/11 \approx 0.36$ , in remarkably good agreement with the experimentally determined value  $\beta \approx 0.36$  in Katgert et al. (2008).

Finally, we point out here that for dense granular media, the main dissipation comes from sliding friction, which could be seen as a viscous interaction with exponent zero — the frictional forces do not change appreciably with the sliding rate. In granular media, it has been taken as a trivality that both the local and global interactions are very similar, namely frictional. We doubt that granular flows are affine, but we believe that this correspondence between local and global flow behavior is a lucky coincidence - we note here that for  $\alpha_{\text{visc}} = 0$ , the global flow exponent  $\beta$  also becomes zero in our model.

## 5.5 Critical collapse

A powerful test of any critical scaling prediction is to plot numerical or experimental data in rescaled coordinates and look for collapse to a master curve. The quality of collapse is a strong test of theory, and the master curve itself is a revealing depiction of the underlying physics. The rheological model described above indeed predicts such master curves, but there is some subtlety owing to the existence of not one but two crossover strain rates.

To illustrate the subtlety, let us first consider an example with only one crossover. The Herschel-Bulkley flow rule contains two regimes, a yield stress regime  $\sigma \approx \sigma_y \sim \Delta\phi^\Delta$  and a critical regime  $\sigma \sim \dot{\gamma}^\beta$ . The crossover between the two regimes occurs at the strain rate  $\dot{\gamma}^*$  for which the two regimes are comparable:  $\dot{\gamma}^* \sim \Delta\phi^{\Delta/\beta}$ . Dividing by  $\Delta\phi^\Delta$ , the Herschel-Bulkley flow rule can be rewritten

$$\frac{\sigma}{\Delta\phi^\Delta} = \text{const} + A \left( \frac{\dot{\gamma}}{\Delta\phi^{\Delta/\beta}} \right)^\beta \quad (16)$$

provided  $A$  does not depend on  $\Delta\phi$  as well [Katgert et al. (2009)]. Note that the term in parentheses is proportional to  $\dot{\gamma}/\dot{\gamma}^*$ , and that all the dependence on  $\Delta\phi$  is contained in the ratios  $\sigma/\Delta\phi^\Delta$  and  $\dot{\gamma}/\Delta\phi^{\Delta/\beta}$ . Therefore *if* the rheology is described by a Herschel-Bulkley rule (or another flow rule with a single crossover rate), plotting the rescaled stress and strain rate,

$$\tilde{\sigma} = \frac{\sigma}{\Delta\phi^\Delta} \quad \text{and} \quad \tilde{\dot{\gamma}} = \frac{\dot{\gamma}}{\Delta\phi^{\Delta/\beta}}, \quad (17)$$

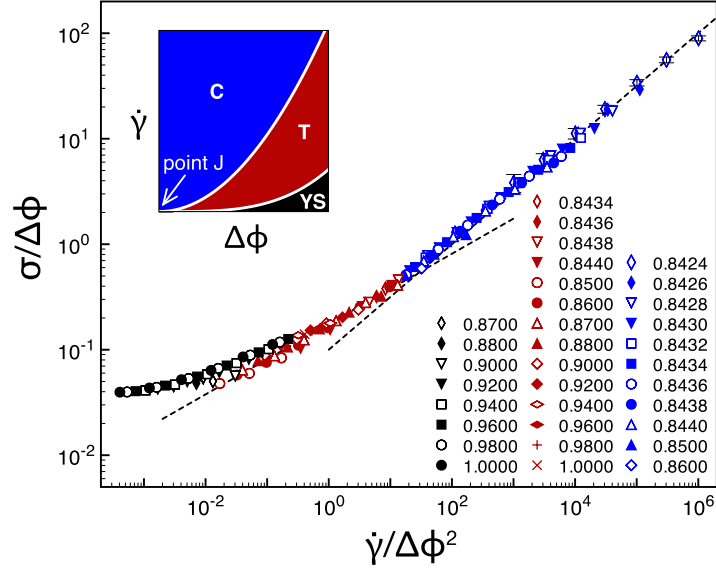


Figure 6: Scaling collapse of flow curves obtained from bubble model simulations as described in Section 5.1. Flow curves are obtained for 4 decades in strain rate and 3 decades in  $\Delta$ , see legend. Rescaled coordinates are  $\sigma/\Delta\phi$  and  $\dot{\gamma}/\Delta\phi^2$ , appropriate for parameters spanning the Transition and Critical regimes. Dashed lines are guides to the eye with slopes 1/3 and 1/2. Inset: Boundaries between the yield stress, transition, and critical regimes in the  $\Delta\phi - \dot{\gamma}$  plane.

should produce collapse to a master curve of the form  $\text{const} + Ax^\beta$ . Alternatively, if the exponents  $\Delta$  and  $\beta$  are unknown, such a scaling plot can be a way to determine them: one looks for the values of  $\Delta$ ,  $\beta$ , and  $\phi_c$  that produce the best data collapse.

Such scaling plots can be made for any curve characterized by two qualitatively different regimes: the first step is always to identify the crossover strain rate (or whatever quantity is on the  $x$ -coordinate). If a curve has more than two regimes, and hence more than one crossover, one generally cannot collapse all data by rescaling with the single scaling parameter  $\Delta\phi$ . The flow model from above predicts not two but three scaling regimes, hence, according to the model, one should not expect to be able to make a scaling plot that collapses all data near  $\phi_c$  for a broad range of  $\dot{\gamma}$ . One can, however, still collapse data from any two adjacent regimes. Consider the Transition and Critical regimes for  $\alpha_{\text{el}} = 1$  and  $\alpha_{\text{visc}} = 1$ , for which  $\sigma \sim \Delta\phi^{1/3}\dot{\gamma}^{1/3}$  and  $\sigma \sim \dot{\gamma}^{1/2}$ , respectively. The crossover rate is  $\dot{\gamma}^* \sim \Delta\phi^2$ , and data from these two regimes should collapse for the rescaled coordinates

$$\tilde{\sigma} = \frac{\sigma}{\Delta\phi} \quad \text{and} \quad \tilde{\dot{\gamma}} = \frac{\dot{\gamma}}{\Delta\phi^2}. \quad (18)$$

This is shown in Fig. 6 and the collapse is indeed very good. Similarly, data from the yield stress and transition regimes can be collapsed by plotting

$$\tilde{\sigma} = \frac{\sigma}{\Delta\phi^{3/2}} \quad \text{and} \quad \tilde{\dot{\gamma}} = \frac{\dot{\gamma}}{\Delta\phi^{7/2}}. \quad (19)$$

Note, however, that generating data in the yield stress regime is numerically challenging; Fig. 6, for example, does not have enough data points in this regime to allow for a convincing test of the model.

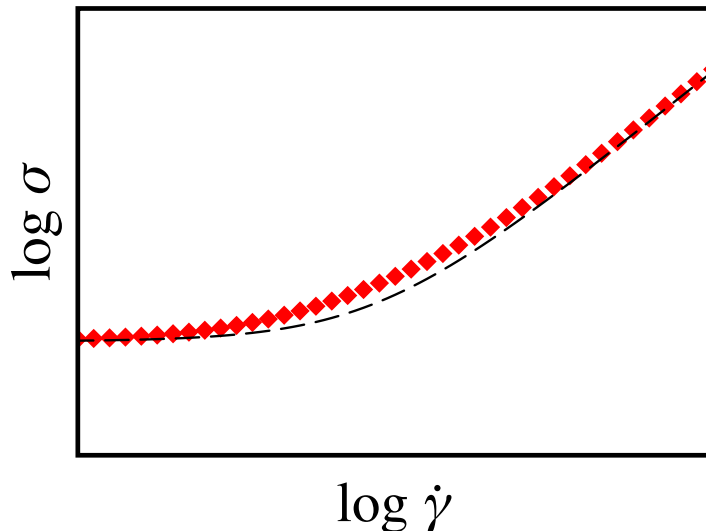


Figure 7: Numerical solution to our scaling model ( $\blacklozenge$ ) and Herschel-Bulkley model with the same asymptotic behaviour (dashed line) compared. The Herschel-Bulkley model underestimates the cross-over as it ignores the Transitional regime.

It is interesting to ask what happens if we attempt to make a scaling plot that assumes a single crossover, as in the Herschel-Bulkley flow rule, when in fact there are multiple crossovers. In effect, this ignores the transition regime, and one should find that data from the transition regime fails to collapse. Fig. 7 shows a plot of data generated by numerically solving our scaling model ( $\alpha_{\text{el}} = \alpha_{\text{visc}} = 1$ ). The dashed line indicates a Herschel-Bulkley law:  $\sigma_y + A\dot{\gamma}^{1/2}$ , with  $\sigma_y$  and  $A$  chosen so as to match the asymptotics of the model. Note that the curve has a soft elbow: the crossover is much slower than the Herschel-Bulkley form would predict. While real experimental data likely are noisy enough to mask the poor collapse in this regime, the soft elbow does appear to be a feature of real flow curves: fits to the HB flow rule typically fare poorly near the crossover point and underestimate the stress, consistent with the existence of a transition regime.

## 5.6 Conclusion and Outlook

In this paper, we have proposed that static and dynamic properties of foams can be captured by recent ideas stemming from jamming - and we have also illustrated how some of these theoretical ideas grew out of experimental questions ("how does a foam lose rigidity") and observations ("fluctuations in foams seem to grow").

We suggest two broad directions for future research. On the one hand, there is a general lack in experimental data confronting some of the predictions, for example in the degree of nonaffinity as a function of wetness [van Hecke (2010)], or the distribution of relative velocity fluctuations as function of strain rate [Tighe et al. (2010)]; more experiments are called for. In particular there are only a handful of studies of the mechanics and flow of very wet foams or emulsions - the recent advent of combined 3D confocal imaging and rheology of emulsions [Zhou et al. (2006); Clusel et al. (2009); Paredes et al. (2011)] should open new experimental avenues to probe the critical regime.

On the other hand, many of the commonly observed phenomena in soft materials are without a

sound description. Here we have focused on steady state rheology, but in practice, oscillatory rheology is the preferred experimental tool to capture the general visco-elastic behavior of soft materials. One of us, has recently developed a theoretical description of linear oscillatory rheology [Tighe (2011)], but there are many other open questions. What is the physics of plastic rearrangements? What is the fate of T1 events when the foam gets increasingly wet? What about memory effects and reversibility [Lundberg et al. (2008)]?

We look forward to many more surprises in the rich physics of collections of bubbles and droplets.

## References

- Argon, A. S. “Plastic deformation in metallic glasses” *Acta Metall.* **27** 47-58 (1979)
- Besseling, R., E. R. Weeks, A. B. Schofield, and W. C. K. Poon, “Three-dimensional imaging of colloidal glasses under steady shear”, *Phys. Rev. Lett.* **99**, 028301 (2007).
- Bolton, F. and D. Weaire, “Rigidity loss transition in a disordered 2D-froth”, *Phys. Rev. Lett.* **65**, 3449 (1990).
- Bretherton, F. P., “The motion of long bubbles in tubes”, *J. Fluid Mech.* **10**, 166-188 (1961).
- Sollich, P, F. Lequeux, P. Hebraud, and M. E. Cates, “Rheology of soft glassy materials ”, *Phys. Rev. Lett.* **78**, 2020-2023 (1997).
- Clusel, M., E. I. Corwin, A. O. N. Siemens, and J. Brujic, “A ‘granocentric’ model for random packing of jammed emulsions”, *Nature* **460**, 611-615 (2009).
- Denkov, N. D., S. Tcholakova, K. Golemanov, K. P. Ananthpadmanabhan, and A. Lips, “The role of surfactant type and bubble surface mobility in foam rheology” *Soft Matter* **5**, 3389-3408 (2009).
- Durian, D. J., “Foam mechanics at the bubble scale”, *Phys. Rev. Lett.* **75**, 4780-4783 (1995).
- Durian, D. J., “Bubble-scale model of foam mechanics: Melting, nonlinear behavior, and avalanches” *Phys. Rev. E* **55**, 1739-1751 (1997).
- Ellenbroek, W. G., Z. Zeravcic, W. van Saarloos, and M. van Hecke, “Non-affine response: Jammed packings vs. spring networks”, *EPL* **87** 34004 (2009).
- Paredes, J., N. Shahidzadeh-Bonn, and D. Bonn, “Shear banding in thixotropic and normal emulsions”, *J. Phys. Cond. Matt.* **23**, 284116 (2011).
- Falk, M. L., and J. S. Langer, “Dynamics of viscoplastic deformation in amorphous solids”, *Phys. Rev. E* **57** 71927205 (1998)
- Hatano, T., “Scaling properties of granular rheology near the jamming transition”, *J. Phys. Soc. Jap.* **77**, 123002 (2008).
- Hatano, T., “Critical scaling of granular rheology”, *Prog. Theor. Phys. Suppl.* **184**, 143 (2010).
- van Hecke M. “Jamming of soft particles: geometry, mechanics, scaling and isostaticity”, *J. Phys. Cond. Matt.* **22**, 033101 (2010).
- Höhler, and S. Cohen-Addad, “Rheology of liquid foam”, *J. Phys. Cond. Matt.* **17**, R1041-R1069 (2005).

- Höhler, R., Y. Y. C. Sang, E. Lorenceau, and S. Cohen-Addad, “Osmotic pressure and structures of monodisperse ordered foam” *Langmuir* **24**, 418-425 (2008).
- Janiaud, E., D. Weaire, and S. Hutzler, “Two-Dimensional foam rheology with viscous drag”, *Phys. Rev. Lett.* **97**, 038302 (2006).
- Katgert, G., M. E. Möbius, and M. van Hecke, “Rate dependence and role of disorder in linearly sheared two-dimensional foams”, *Phys. Rev. Lett.* **101**, 058301 (2008).
- Katgert, G., A. Latka, M. E. Möbius, and M. van Hecke, “Flow in linearly sheared two-dimensional foams: from bubble to bulk scale”, *Phys. Rev. E* **79**, 066318 (2009).
- Katgert, G., and M. van Hecke, “Jamming and geometry of two-dimensional foams”, *EPL* **92**, 34002 (2010).
- Kraynik, A. M., “Foam flows”, *Ann. Rev. Fluid Mech.* **20**, 325-357 (1988).
- Lacasse, M.-D., G. S. Grest, D. Levine, T. G. Mason, and D. A. Weitz, “Model for the elasticity of compressed emulsions”, *Phys. Rev. Lett.* **76**, 3448-3451 (1996).
- Langlois, V. J., S. Hutzler, and D. Weaire, “Rheological properties of the soft-disk model of two-dimensional foams”, *Phys. Rev. E* **78**, 021401 (2008).
- Larson R. G., “The structure and rheology of complex fluids”, Oxford University Press, New York, (1999).
- Lemaître, A., and C. Maloney, “Sum rules for the quasi-static and visco-elastic response of disordered solids at zero temperature”, *J. Stat. Phys.* **123**, 415-453 (2006).
- Lespiat, R., S. Cohen-Addad, and R. Höhler, “Jamming and flow of random-close-packed spherical bubbles: An analogy with granular materials”, *Phys. Rev. Lett.* **106**, 148302 (2011).
- Liu, A. J., and S. R. Nagel, “Nonlinear dynamics: Jamming is not just cool any more”, *Nature* **396**, 21-22 (1998).
- Liu, A. J., and S. R. Nagel, “The jamming transition and the marginally jammed solid”, *Ann. Rev. Cond. Matt. Phys.* **1**, 347-369 (2010).
- Lundberg, M., K. Krishan, N. Xu, C. S. O’Hern, and M. Dennin, “Reversible plastic events in amorphous materials” *Phys. Rev. E* **77**, 041505 (2008).
- Majmudar, T. S., M. Sperl, S. Luding, and R. P. Behringer, “Jamming transition in granular systems”, *Phys. Rev. Lett.* **98**, 058001 (2007).
- Maloney, C. E., “Correlations in the elastic response of dense random packings”, *Phys. Rev. Lett.* **97**, 035503 (2006).
- Mason, T. G., J. Bibette, and D. A. Weitz, “Elasticity of compressed emulsions”, *Phys. Rev. Lett.* **75**, 2051-2054 (1995).
- Mason, T. G., J. Bibette, and D. A. Weitz, “Yielding and flow of monodisperse emulsions”, *J. Coll. Int. Sc.* **179**, 439-448 (1996).
- Mason, T. G., M.-D. Lacasse, G. S. Grest, D. Levine, J. Bibette, and D. A. Weitz, “Osmotic pressure and viscoelastic shear moduli of concentrated emulsions”, *Phys. Rev. E* **56**, 3150-3166 (1997).

- Möbius, M. E., G. Katgert, and M. van Hecke, “Relaxation and flow in linearly sheared two-dimensional foams”, *EPL* **90**, 44003 (2010).
- Nordstrom, K. N., E. Verneuil, P. E. Arratia, A. Basu, Z. Zhang, A. G. Yodh, J. P. Gollub, and D. J. Durian, “Microfluidic rheology of soft colloids above and below Jamming”, *Phys. Rev. Lett.* **105**, 175701 (2010).
- Nordstrom, K. N., E. Verneuil, W. G. Ellenbroek, T. C. Lubensky, J. P. Gollub, and D. J. Durian, “Centrifugal compression of soft particle packings: Theory and experiment”, *Phys. Rev. E* **82**, 041403 (2010).
- O’Hern, C. S., L. E. Silbert, A. J. Liu, and S. R. Nagel, “Jamming at zero temperature and zero applied stress: The epitome of disorder” *Phys. Rev. E* **68**, 011306 (2003).
- Olsson, P., and S. Teitel, “Critical scaling of shear viscosity at the jamming transition.”, *Phys. Rev. Lett.* **99**, 178001 (2007).
- Otsuki, M., and H. Hayakawa, “Universal scaling for the Jamming transition”, *Prog. Theor. Phys.* **121**, 647-655 (2009).
- Ono, I. K., C. S. O’Hern, D. J. Durian, S. A. Langer, A. J. Liu, and S. R. Nagel, “Effective temperatures of a driven system near Jamming”, *Phys. Rev. Lett.* **89**, 095703 (2002).
- Princen, H. M., “Rheology of foams and highly concentrated emulsions. 1. Elastic properties and yield stress of a cylindrical model system”, *J. Coll. Int. Sc.* **91**, 160-175 (1983).
- Princen, H. M., and A. D Kiss, “Rheology of foams and highly concentrated emulsions. 3. Static shear modulus”, *J. Coll. Int. Sc.* **112**, 427-437 (1986).
- Radjai, F., and S. Roux, “Turbulentlike fluctuations in quasistatic flow of granular media”, *Phys. Rev. Lett.* **89**, 064302 (2002).
- Schall, P., and M. van Hecke, “Shear bands in matter with granularity”, *Ann. Rev. Fluid Mech.* **42**, 67-88 (2010).
- Somfai, E., J.-N. Roux, J. H. Snoeijer, M. van Hecke, and W. Van Saarloos, “Elastic wave propagation in confined granular systems”, *Phys. Rev. E* **72**, 021301 (2005).
- Saint-Jalmes, A., and D. J. Durian, “Vanishing elasticity for wet foams : Equivalence with emulsions and role of polydispersity”, *J. Rheol.* **43**, 1411-1422 (1999).
- Tanguy, A., J. P. Wittmer, F. Leonforte, and J. L. Barrat, “Continuum limit of amorphous elastic bodies: A finite-size study of low-frequency harmonic vibrations”, *Phys. Rev. B* **66**, 174205 (2002).
- Tanguy, A., F. Leonforte, J. P. Wittmer, and J. L. Barrat, “Vibrations of amorphous nanometric structures: when does the classical continuum theory apply?”, *App. Surf. Sci.* **226**, 282-288 (2004).
- Tewari, S., D. Schiemann, D. J. Durian, C. M. Knobler, S.A. Langer, and A. J. Liu, “Statistics of shear-induced rearrangements in a two-dimensional model foam”, *Phys. Rev. E* **60** 4385-4396 (1999).

- Tighe, B. P., E. Woldhuis, J. J. C. Remmers, W. van Saarloos, and M. van Hecke, “Model for the scaling of stresses and fluctuations in flows near Jamming” *Phys. Rev. Lett.* **105**, 088303 (2010).
- Tighe, B. P., “Relaxations and rheology near jamming”, to appear in *Phys. Rev. Lett.* (2011).
- Wang, Y., K. Krishan, and M. Dennin, “Impact of boundaries on velocity profiles in bubble rafts”, *Phys. Rev. E* **73**, 031401 (2006).
- Weitz, D., “Packing in the spheres” *Science* **303**, 968-969 (2004).
- Weaire, D., and S. Hutzler, “The physics of foams”, Clarendon Press, Oxford, (1999).
- Wyart, M., H. Liang, A. Kabla, and L. Mahadevan, “Elasticity of floppy and stiff random networks”, *Phys. Rev. Lett.* **101**, 215501 (2008).
- Zhou, J., S. Long, Q. Wang, and A. D. Dinsmore, “Measurement of forces inside a three-dimensional pile of frictionless droplets”, *Science* **312**, 1631-1633 (2006).